JCCS-PFGM: A Novel Circle-Supervision Based Poisson Flow Generative Model for Multiphase CECT Progressive Low-Dose Reconstruction with Joint Condition

Rongjun Ge[1], Yuting He[2], Cong Xia[3], and Daoqiang Zhang[4](✉)

[1] School of Instrument Science and Engineering, Southeast University, Nanjing, China
[2] School of Computer Science and Engineering, Southeast University, Nanjing, China
[3] Jiangsu Key Laboratory of Molecular and Functional Imaging, Department of Radiology, Zhongda Hospital, Medical School of Southeast University, Nanjing, China
[4] College of Computer Science and Technology, Nanjing University of Aeronautics and Astronautics, Nanjing, China
dqzhang@nuaa.edu.cn

Abstract. Multiphase contrast-enhanced computed tomography (CECT) scan is clinically significant to demonstrate the anatomy at different phases. But such multiphase scans inherently lead to the accumulation of huge radiation dose for patients, and directly reducing the scanning dose dramatically decrease the readability of the imaging. Therefore, guided with **J**oint **C**ondition, a novel **C**ircle-**S**upervision based **P**oisson **F**low **G**enerative **M**odel (JCCS-PFGM) is proposed to promote the progressive low-dose reconstruction for multiphase CECT. JCCS-PFGM is constituted by three special designs: 1) a progressive low-dose reconstruction mechanism to leverages the imaging consistency and radiocontrast evolution along former-latter phases, so that enormously reduces the radiation dose needs and improve the reconstruction effect, even for the latter-phase scanning with extremely low dose; 2) a circle-supervision strategy embedded in PFGM to enhance the refactoring capabilities of normalized poisson field learned from the perturbed space to the specified CT image space, so that boosts the explicit reconstruction for noise reduction; 3) a joint condition to explore correlation between former phases and current phase, so that extracts the complementary information for current noisy CECT and guides the reverse process of diffusion jointly with multiphase condition for structure maintenance. The extensive experiments tested on the clinical dataset composed of 11436 images show that our JCCS-PFGM achieves promising PSNR up to 46.3dB, SSIM up to 98.5%, and MAE down to 9.67 HU averagely on phases I, II and III, in quantitative evaluations, as well as

Supplementary Information The online version contains supplementary material available at https://doi.org/10.1007/978-3-031-43999-5_39.

H. Greenspan et al. (Eds.): MICCAI 2023, LNCS 14229, pp. 409–418, 2023.
https://doi.org/10.1007/978-3-031-43999-5_39

gains high-quality readable visualizations in qualitative assessments. All of these findings reveal our method a great potential in clinical multi-phase CECT imaging.

1 Introduction

The substantial reduction of scanning radiation dose and its accurate reconstruction are of great clinical significance for multiphase contrast-enhanced computed tomography (CECT) imaging. 1) Multiphase CECT requires multiple scans at different phases, such as arterial phase, venous phase, delayed phase and etc., to demonstrate the anatomy and lesion with the contrast agent evolution intra human body over time [1]. But such multiphase scans inherently lead to the accumulation of huge radiation dose for patients [2,3]. As shown in Fig. 1(a), after triple-phase CECT scanning, the radiation damage suffered by the patient is three times that of the single phase. Combined with "as low as reasonably achievable" (ALARA) principle [4], it is thus extremely urgent to greatly reduce the radiation dose and risk for clinical multiphase CECT examination. 2) However, the low-dose acquired CT image also exists the problems of noise interference and unclear structure. As enlarged region shown in Fig. 1(b), the low-dose CECT behaves much lower signal-to-noise ratio than normal-dose CECT. It brings great difficulty to read the anatomical structure with high noise, especially for inexperienced radiologist. Therefore, the high-quality reconstruction with more readable pattern is clinically crucial for multi-phase low-dose CECT diagnosis.

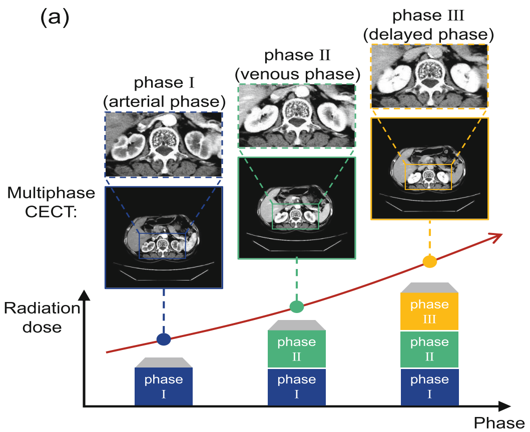

Fig. 1. (a) Multiphase CECT scans comprehensively enable the demonstration of anatomy and lesion with the contrast agent evolution at different phases, but inherently lead to the accumulation of huge radiation dose for patients. (b) Low-dose CECT effectively reduce the radiation risk, but it causes difficulty to read the anatomical structure with high noise, compared to normal-dose CECT.

As far as we know, most of the existing methods mainly focus on the single-phase low-dose CT (LDCT) reconstruction. Chen et al. [5] trained a deep CNN to transform LDCT images towards normal-dose CT images, patch by patch. In [6], a shortcut connections aided symmetrical CNN was adopt to predict noise distribution in LDCT. Shan et al. [7] attempted to transfer a trained 2D CNN to a 3D counterpart for low-dose CT image denoising. In [8], an attention residual dense network was developed for LDCT sinogram data denoising. In [9], low-dose sinogram- and image- domain networks were trained in a progressive way. Zhang et al. [10] further connected sinogram- and image- domain networks together for joint training. In [11] and [12], parallel network architectures were put forward for dual-domain information exchange and mutual optimization.

Multi-phase low-dose CT reconstruction is still ignored, though single-phase methods behave promising results on their issues [5–12]. Due to multiple scans in a short time, it has the inherent challenges: 1) The serious noise pollution is caused by the higher requirement of using much lower scanning dose to decrease multiphase radiation accumulation, compared to the single-phase imaging. Thus, how to elegantly learn such mapping relation from the lower-dose CECT with more serious noise to normal-dose CECT is extremely critical. 2) Complex multiphase correlation with redundancy and interference is induced by the evolution of contrast agent in the human body. Except redundancy and interference, strong causality also obviously exists among multiphase. But how to deeply explore such consistency and evolution along the multiphase for further reducing the dose of later phase and improving imaging quality is still an open challenge.

In this paper, guided with **J**oint **C**ondition, a novel **C**ircle-**S**upervision based **P**oisson **F**low **G**enerative **M**odel (JCCS-PFGM) is proposed to make the progressive low-dose reconstruction for multiphase CECT. It deeply explores the correlation among multiphase and the mapping learning of PFGM, to progressively reduce the scanning radiation dose of multiphase CECT to the ultra low level of 5% dose, and achieve the high-quality reconstruction with noise reduction and structure maintenance. It thus significantly reduces the radiation risk of multiple CT scans in a short time, accompanied with clear multiphase CECT examination images. The main contributions of JCCS-PFGM can be summarized as: 1) an effectively progressive low-dose reconstruction mechanism is developed to leverages the imaging consistency and radiocontrast evolution along former-latter phases, so that enormously reduces the radiation dose needs and improve the reconstruction effect, even for the latter-phase scanning with extremely low dose; 2) a newly-designed circle-supervision strategy is proposed in PFGM to enhance the refactoring capabilities of normalized poisson field learned from the perturbed space to the specified CT image space, so that boosts the explicit reconstruction for noise reduction; 3) a novel joint condition is designed to explore correlation between former phases and current phase, so that extracts the complementary information for current noisy CECT and guides the reverse process of diffusion jointly with multiphase condition for structure maintenance.

2 Methodology

As shown in Fig. 2, the proposed JCCS-PFGM is progressively performed on multiphase low-dose CECT to reduce the radiation risk in multiple CT imaging and make the high-quality reconstruction with noise reduction and structure maintenance. It is conducted with three special designs: 1) the progressive low-dose reconstruction mechanism (detailed in Sect. 2.1) reasonably utilizes the consistency along the multiphase CECT imaging, via phase-by-phase reducing the radiation dose and introducing the priori knowledge from former-phase reconstruction; 2) the circle-supervision strategy (detailed in Sect. 2.2) embedded in PFGM makes further self-inspection on normal poisson field prediction, via penalizing the deviation between the same-perturbed secondary diffusion; and 3) the joint condition (detailed in Sect. 2.3) integrates the multi-phase consistency and evolution in guiding the reverse process of diffusion, via fusing the complementary information from former phases into current ultra low-dose CECT.

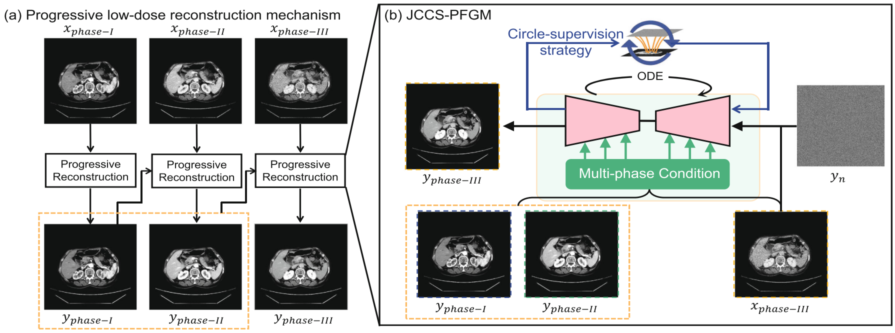

Fig. 2. JCCS-PFGM promotes the progressive low-dose reconstruction for multiphase CECT. It is composed by progressive low-dose reconstruction mechanism, circle-supervision strategy and joint condition.

2.1 Progressive Low-Dose Reconstruction Mechanism

The progressive low-dose reconstruction mechanism effectively promotes high-level base from former-phase to latter-phase for successively multiphase CECT reconstruction, instead of the casually equal dose reduction seriously breaking the structure in each phase. It further exploits the inherent consistency traceable along multiphase CECT to reduce the burden of multiphase reconstruction.

As show in Fig. 2(a), the reasonable-designed progressive low-dose reconstruction mechanism arranges the dose from relatively high to low along the causal multiphase of phases I, II and III. With such mechanism, the reconstruction of former phase acquire more scanning information, benefit from relatively high dose. And the latter phase is granted with much more reliable priori knowledge, benefit from the consistently traceable former-phase reconstruction. Denote the low-dose CECT at phases I, II and III as $x_{phase-I}$, $x_{phase-II}$ and $x_{phase-III}$, the procedure is formulated as:

$$\begin{cases} y_{phase-I} = \mathcal{R}_1(x_{phase-I}) \\ y_{phase-II} = \mathcal{R}_2(x_{phase-II}, y_{phase-I}) \\ y_{phase-III} = \mathcal{R}_3(x_{phase-III}, [y_{phase-II}, y_{phase-I}]) \end{cases} \tag{1}$$

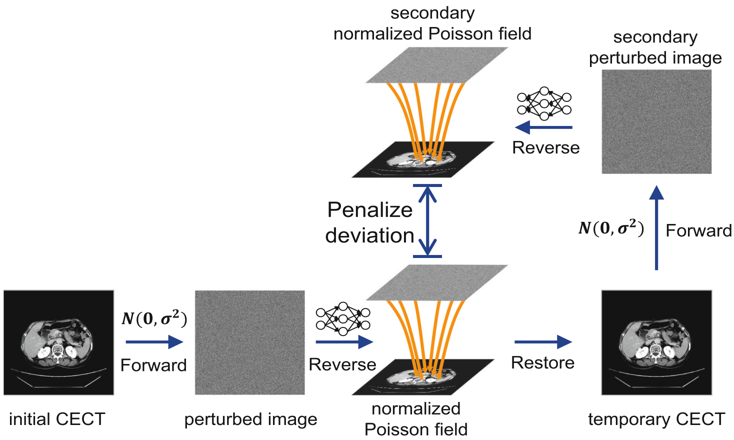

Fig. 3. The circle-supervision strategy robustly boosts the refactoring capabilities of normalized Poisson field learned by PFGM, via penalizing the deviation between the same-perturbed secondary diffusion.

where $y_{phase-I}$, $y_{phase-II}$ and $y_{phase-III}$ represent reconstruction result, as well as $\mathcal{R}_1(\cdot)$, $\mathcal{R}_2(\cdot)$ and $\mathcal{R}_3(\cdot)$ mean reconstruction model.

2.2 Circle-Supervision Strategy Embedded in PFGM

The circle-supervision strategy robustly boosts the refactoring capabilities of normalized Poisson field learned by PFGM. So that it further promotes the explicit reconstruction for noise reduction, instead of just CT-similar image generation.

PFGM is good at mapping a uniform distribution on a high-dimensional hemisphere into any data distribution [13]. It is inspired by electrostatics, and interpret initial image data points as electrical charges on the $z = 0$ hyperplane. Thus the initial image is able to be transformed into a uniform distribution on the hemisphere with radius $r \to \infty$. It estimates normalized Poisson field with deep neural network (DNN) and thus further uses backward ordinary differential equation (ODE) to accelerate sampling.

Here, we further propose the circle-supervision strategy on the normalized Poisson field which reflects the mapping direction from the perturbed space to the specified CT image space. It remedies the precise perception on the target initial CECT besides mapping direction learning, to enhance the crucial field components. As shown in Fig. 3, after randomly yield perturbed image through forward process, the DNN estimates the normalized Poisson field ϕ_1. Then according to the normalized field calculation in the forward process, the Poisson field is returned with denormalization operation, and further temporarily restore the perturbed image into the initial CECT space. The secondary diffusion is conducted with same perturbtion in forward process and DNN in reverse process. Finally, the normal Poisson field of the secondary diffusion ϕ_2 is estimated. The deviation between ϕ_1 and ϕ_2 is penalized to boost the refactoring capabilities. Besides the temporary CECT is also yield in the secondary diffusion to enhance the robustness.

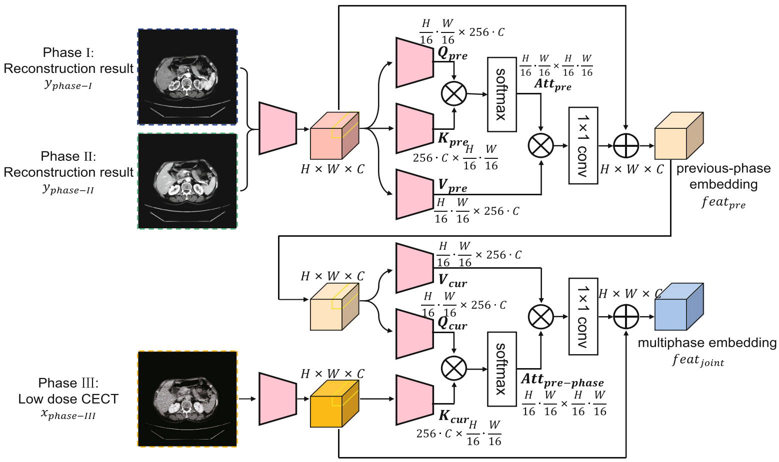

Fig. 4. The joint condition comprehensively fuses the consistency and evolution from the former phases to enhance the current ultra low-dose CECT (take the phase III low-dose CECT reconstruction for example). It is composed of self-fusion among former phases for consistency, and cross-fusion between former and current phases for evolution.

2.3 Joint Condition Fusing Multiphase Consistency and Evolution

The joint condition comprehensively fuses the consistency and evolution from the previous phases to enhance the current ultra low-dose CECT. With such multiphase fusion, the reverse process of diffusion is able to get the successive guide to perceive radiocontrast evolution for structure maintenance

As shown in Fig. 4, the joint condition consists of two parts: the self-fusion among previous phases for consistency and the cross-fusion between previous

Table 1. The quantitative analysis of the proposed method under different configurations. (PLDRM: Progressive low-dose reconstruction mechanism with direct concatenation, CS: Circle-supervision strategy)

Method	Phase I (30%dose)			Phase II (15%dose)			Phase III (5%dose)		
	MAE (↓)	PSNR (↑)	SSIM (↑)	MAE (↓)	PSNR (↑)	SSIM (↑)	MAE (↓)	PSNR (↑)	SSIM (↑)
PFGM	7.80HU	47.4 db	97.3%	10.3HU	44.8 db	97.1%	16.0HU	42.5 db	96.8%
+PLDRM	7.80HU	47.4 db	97.3%	9.7HU	45.3 db	97.7%	15.3HU	43.1 db	97.2%
+CS	7.23HU	47.9 db	98.0%	9.2HU	45.6 db	98.0%	14.8HU	43.8 db	97.5%
Ours	**6.12HU**	**48.4 db**	**98.8%**	**8.49HU**	**46.0 db**	**98.7%**	**14.4HU**	**44.7 db**	**98.0%**

Table 2. The quantitative analysis of the proposed method compared with the existing methods.

Method	Phase I (30%dose)			Phase II (15%dose)			Phase III (5%dose)		
	MAE (↓)	PSNR (↑)	SSIM (↑)	MAE (↓)	PSNR (↑)	SSIM (↑)	MAE (↓)	PSNR (↑)	SSIM (↑)
FBP	15.78HU	40.1 db	93.9%	21.5HU	37.6 db	89.2%	34.9HU	33.7 db	77.9%
RED-CNN	7.76HU	47.0 db	97.7%	11.8HU	44.2 db	96.2%	18.6HU	42.2 db	95.4%
CLEAR	8.61HU	45.9 db	96.2%	10.1HU	45.4 db	97.4%	19.7HU	41.5 db	95.9%
DDPNet	8.07HU	46.8 db	97.5%	10.4HU	45.8 db	98.0%	16.8HU	42.7 db	97.1%
Ours	**6.12HU**	**48.4 db**	**98.8%**	**8.49HU**	**46.0 db**	**98.7%**	**14.4HU**	**44.7 db**	**98.0%**

and current phases for evolution. 1) For the self-fusion among former phases, it firstly encodes the combination of the reconstruction results of the previous phase I $y_{phase-I}$ and phase II $y_{phase-II}$ into the feature domain. And key map K_{pre}, query map Q_{pre} and value map V_{pre} are then generated with further encoder and permutation. K_{pre} and Q_{pre} together establish the correlation weight, i.e., attention map Att_{pre}, among former phases combination to explore the inherent consistency. Att_{pre} further works on the value map V_{pre} to extract the consistent information which is finally added on the first feature representation to get previous-phases embedding $feat_{pre}$. The procedure is formulated as:

$$\begin{cases} K_{pre} = E_{K-pre}(E_{pre}([y_{phase-I}, y_{phase-II}])) \\ Q_{pre} = E_{Q-pre}(E_{pre}([y_{phase-I}, y_{phase-II}])) \\ V_{pre} = E_{V-pre}(E_{pre}([y_{phase-I}, y_{phase-II}])) \\ feat_{pre} = Conv(Softmax(Q_{pre}K_{pre}/\sqrt{d})V_{pre}) + E_{pre}([y_{phase-I}, y_{phase-II}]) \end{cases} \tag{2}$$

where $E_{pre}(\cdot)$,$E_{K-pre}(\cdot)$,$E_{Q-pre}(\cdot)$ and $E_{V-pre}(\cdot)$ are encoders, $Softmax(\cdot)$ means Softmax function, and $Conv((\cdot)$ represents 1×1 convolution.

2) For the cross-fusion between previous and current phases, it uses $feat_{pre}$ to generate query map Q_{cur} and value map V_{cur}. The current phase III low-dose CECT $x_{phase-III}$ is encoded for key map K_{cur}. Thus the evolution between the current phase and previous phases is explored between K_{cur} and Q_{cur} by attention map Att_{cur}. Then complimentary evolution from previous phases is extracted from value map V_{cur} with Att_{cur}, and then added into the current

phase. The procedure is formulated as:

$$\begin{cases} K_{cur} = E_{K-cur}(E_{cur}(x_{phase-III})) \\ Q_{cur} = E_{Q-cur}(feat_{pre}) \\ V_{cur} = E_{V-cur}(feat_{pre}) \\ feat_{cur} = Conv(Softmax(Q_{cur}K_{cur}/\sqrt{d})V_{cur}) + E_{cur}(x_{phase-III}) \end{cases} \tag{3}$$

3 Experiments

3.1 Materials and Configurations

A clinical dataset consists 38496 CECT images from 247 patient are used in the experiment. Each patient has triple-phase CECT. We randomly divide the dataset into 123 patients' CECT for training, 49 for validation, and 75 for testing. The basic DNN used in reverse process is same as PFGM. The joint condition is introduced in DNN by making cross attention with DNN feature. Mean Absolute Error (MAE), SSIM and Peak Signal-to-Noise- Ratio(PSNR) are used to evaluate the performance. The corresponding multiphase low-dose CECT is simulated by validated photon-counting model that incorporates the effect of the bowtie filter, automatic exposure control, and electronic noise [14].

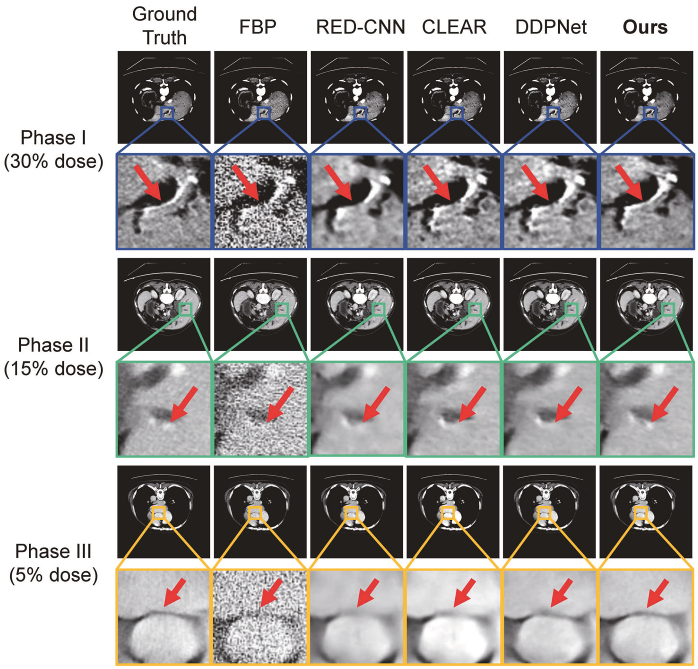

Fig. 5. Visual comparison with competing methods, the proposed JCCS-PFGM effectively keeps structural subtitles in all phases.

3.2 Results and Analysis

Overall Performance. As the last column shown in Table 1 and Table 2, the proposed JCCS-PFGM achieves high-quality multiphase low-dose CECT reconstruction with MAE down to 9.67 HU for information recovery, PSNR up to 46.3 dB for noise reduction, and SSIM up to 98.5% for structure maintaince, averagely on phases I, II and III.

Ablation Study. As shown in Table 1, the proposed JCCS-PFGM gains error decrease of 1.23HU, as well as increase of 1.05 dB PSNR and 1.06% SSIM, in average, compared to the basic PFGM with current-phase condition, and various configurations by successively adding progressive low-dose reconstruction mechanism and circle-supervision strategy. It reveals the effect of each special design. Especially for phase III with ultra low dose of 5%, it gets great improvement.

Comparison with Competing Methods. As shown in Table 2, the proposed JCCS-PFGM gains the best performance compared to FBP, RED-CNN [5], CLEAR [10] and DDPNet [12], with error decrease of 5.66 HU, PSNR increase of 3.62dB PSNR and SSIM improvement by 3.88% on average. Visually, Fig. 5 illustrates that the result from JCCS-PFGM preserved tiny structure in all the phases with the dose assignment scheme: phase I 30% of the total nominal dose, phase II 15% and phase III 5%. In the enlarged ROI where the interpretation is difficult with original LDCT images, our method revealed key details, such as the vessel indicated by the red arrow, much better than the compared methods.

4 Conclusion

In this paper, we propose JCCS-PFGM to make the progressive low-dose reconstruction for multiphase CECT. JCCS-PFGM t creatively consists of 1) the progressive low-dose reconstruction mechanism utilizes the consistency along the multiphase CECT imaging; 2) the circle-supervision strategy embedded in PFGM makes further self-inspection on normal poisson field prediction; 3) the joint condition integrates the multi-phase consistency and evolution in guiding the reverse process of diffusion. Extensive experiments with promising results from both quantitative evaluations and qualitative assessments reveal our method a great clinical potential in CT imaging.

Acknowledgements. This study was supported by Natural Science Foundation of Jiangsu Province (No. BK20210291), National Natural Science Foundation (No. 62101249), China Postdoctoral Science Foundation (No. 2021TQ0149, 2022M721611).

References

1. Meng, X.P., et al.: Radiomics analysis on multiphase contrast-enhanced CT: a survival prediction tool in patients with hepatocellular carcinoma undergoing transarterial chemoembolization. Front. Oncol. **10**, 1196 (2020)
2. Brenner, D.J., Hall, E.J.: Computed tomography an increasing source of radiation exposure. New England J. Med. **357**(22), 2277–2284 (2007)

3. Rastogi, S., et al.: Use of multiphase CT protocols in 18 countries: appropriateness and radiation doses. Can. Assoc. Radiol. J. **72**(3), 381–387 (2021)
4. Prasad, K.N., Cole, W.C., Haase, G.M.: Radiation protection in humans: extending the concept of as low as reasonably achievable (ALARA) from dose to biological damage. Br. J. Radiol. **77**(914), 97–99 (2004)
5. Chen, H., et al.: Low-dose CT denoising with convolutional neural network. In: 14th International Symposium on Biomedical Imaging (ISBI 2017), pp. 143–146. IEEE, Melbourne (2017)
6. Chen, H., et al.: Low-dose CT with a residual encoder-decoder convolutional neural network. IEEE Trans. Med. Imaging **36**(12), 2524–2535 (2017)
7. Shan, H., Zhang, Y., Yang, Q., Kruger, U., Kalra, M.K., Wang, G.: 3-D convolutional encoder-decoder network for low-dose CT via transfer learning from a 2-D trained network. IEEE Trans. Med. Imaging **37**(6), 1522–1534 (2018)
8. Ma, Y.J., Ren, Y., Feng, P., He, P., Guo, X.D., Wei, B.: Sinogram denoising via attention residual dense convolutional neural network for low-dose computed tomography. Nucl. Sci. Tech. **32**(4), 1–14 (2021)
9. Yin, X., et al.: Domain progressive 3D residual convolution network to improve low-dose CT imaging. IEEE Trans. Med. Imaging **38**(12), 2903–2913 (2019)
10. Zhang, Y., et al.: CLEAR: comprehensive learning enabled adversarial reconstruction for subtle structure enhanced low-dose CT imaging. IEEE Trans. Med. Imaging **40**(11), 3089–3101 (2021)
11. Ye, X., Sun, Z., Xu, R., Wang, Z., Li, H.: Low-dose CT reconstruction via dual-domain learning and controllable modulation. In: Wang, L., Dou, Q., Fletcher, P.T., Speidel, S., Li, S. (eds.) MICCAI 2022. LNCS, vol. 13436, pp. 549–559. Springer, Cham (2022). https://doi.org/10.1007/978-3-031-16446-0_52
12. Ge, R., et al.: DDPNet: a novel dual-domain parallel network for low-dose CT reconstruction. In: Wang, L., Dou, Q., Fletcher, P.T., Speidel, S., Li, S. (eds.) MICCAI 2022. LNCS, vol. 13436, pp. 748–757. Springer, Cham (2022). https://doi.org/10.1007/978-3-031-16446-0_71
13. Xu, Y., Liu, Z., Tegmark, M., Jaakkola, T. S.: Poisson flow generative models. In: Advances in Neural Information Processing Systems (2022)
14. Yu, L., Shiung, M., Jondal, D., McCollough, C.H.: Development and validation of a practical lower-dose-simulation tool for optimizing computed tomography scan protocols. J. Comput. Assist. Tomogr. **36**(4), 477–487 (2012)